Dressed-state mixed-parity transitions for realizing negative refractive index

Clifford M. Krowne[1] and Jian Qi Shen[2]
[1]*Microwave Technology Branch, Electronics Science & Technology Division, Naval Research Laboratory, Washington, DC 20375-5347, USA*
[2]*Center for Optical and Electromagnetic Research, Zhejiang University, East Building No. 5, Zijingang Campus, Hangzhou 310058, The People's Republic of China*

(Received 14 August 2008; revised manuscript received 24 November 2008; published 17 February 2009)

The dressed states that are linear combinations of two bare levels of an atom (e.g., an alkali-metal atom) can be realized by a strong-coupling laser beam. As the dressed states have mixed parities, both electric- and magnetic-dipole-allowed transitions can occur between the dressed states and a third level with a definite (pure) parity. It is shown that such dressed-state mixed-parity transitions in an atomic vapor (the concept also applies in the solid state) can give rise to a negative refractive index. The produced negative refractive index is isotropic with atomic-scale microscopic structure units, and the negative real part can emerge in the optical frequency band. Also examined is the case of a fully quantized probe photonic field which interrogates the bottom dressed state and the third-level state. Similarities between the semiclassical approach for the weaker probe field and its fully quantum mechanical second-quantization treatment are discussed in regard to the off-diagonal density matrix element for the reduced 2×2 manifold, and its implications for the refractive index.

DOI: 10.1103/PhysRevA.79.023818 PACS number(s): 42.50.Nn, 32.10.Dk, 33.15.Kr

I. INTRODUCTION

Over the last decade, a new type of artificial metamaterial, whose electric permittivity and magnetic permeability are simultaneously negative in certain frequency bands, has captured extensive attention from many researchers in various fields (e.g., see [1–4]). It can be readily verified that a medium will have a negative refractive index if its permittivity and permeability are simultaneously negative. These metamaterials, which are now known as left-handed media, exhibit a number of interesting electromagnetic and optical effects, including the reversals of both Doppler shift and Cherenkov radiation [1], anomalous refraction [1], amplification of evanescent waves [3] (and hence subwavelength focusing [3,5]), a negative Goos-Hänchen shift [6], a reversed circular Bragg phenomenon [7], photon helicity inversion [8], some unusual photon tunneling effects [9], reversed H field circulation patterns and inverted E field lines in propagating structures [10], and switched field intensity locations in anisotropic transmission structures [11]. Recently, simultaneous negative permittivity and permeability have been achieved experimentally in microwave frequency regions with a composite stucture formed by an array of long metallic wires and an array of split ring resonators [2,12–15]. Although Veselago's original paper [1] and most of the recent theoretical work investigated *isotropic* left-handed media [13], yet, up to now, the left-handed media that have been designed and fabricated successfully for experiments are actually *anisotropic* in nature, and at present it may be somewhat difficult to prepare an isotropic left-handed medium [16–18]. Obviously, the impact would be enormous if an *isotropic* and *homogeneous* material of negative refractive index (with microscopic structure units at the atomic scale level) could be realized in *optical frequency domains* by using a quantum optical approach. Here, we suggest a scheme to realize a negative refractive index in an atomic vapor (the concept should also be applicable to solid state media) where the left-handed vapor produced is isotropic.

Within the last few years, there have been a number of techniques to realize negative refraction, including artificial composite metamaterials [2,12,13], photonic crystal structures [19–21], chiral or chiral mixture materials [22–25], and transmission line simulation [26], for example. All these techniques were proposed within the framework of classical electromagnetic theory. However, the atomic vapor medium with negative indices presented here is based on a quantum optical mechanism. In our method, the dressed-state mixed-parity transitions that can give rise to both electric and magnetic responses are utilized to realize left-handedness of a probe light. In the schematic diagram depicted in Fig. 1, the electric-dipole-allowed transition $|a\rangle$-$|b\rangle$ is driven by a

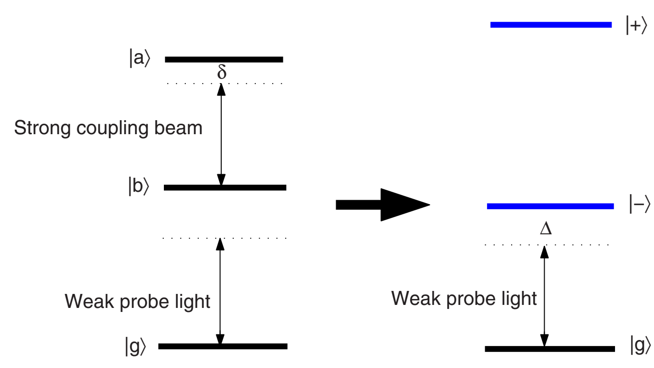

FIG. 1. (Color online) Three-level energy band diagram for the dressed-state mixed-parity transition system. The electric-dipole-allowed transition $|a\rangle$-$|b\rangle$ is driven by a strong-coupling laser beam, and two dressed states $|+\rangle$ and $|-\rangle$ will result from linear combinations of the two bare-state levels $|a\rangle$ and $|b\rangle$. The energy level pair $|g\rangle$-$|-\rangle$ is coupled to the probe electric and magnetic fields. Both electric- and magnetic-dipole-allowed transitions between the ground level $|g\rangle$ and the mixed-parity dressed level $|-\rangle$ emerge, if the probe light excites the $|g\rangle$-$|-\rangle$ transition.

strong-coupling laser beam, and this leads to two orthogonal dressed states $|+\rangle$ and $|-\rangle$, which are linear combinations of the two bare levels $|a\rangle$ and $|b\rangle$. As the lower dressed state $|-\rangle$ possesses a mixed parity, both electric- and magnetic-dipole-allowed transitions between $|g\rangle$ and $|-\rangle$ will emerge, if the pair $|g\rangle-|-\rangle$ is coupled to the electric and magnetic fields of a probe beam.

In the sections that follow, we study dressed-state mixed-parity transitions (Sec. II with ramifications of a quantized photonic probe beam in Sec. III), and obtain the atomic microscopic electric and magnetic polarizabilities (Sec. IV), and then present an illustrative example (in Sec. VI, after finding the negative refractive index branches in Sec. V) to show the existence of the negative refractive index in the vapor medium. Concluding remarks are in Sec. VII.

II. DRESSED-STATE MIXED-PARITY TRANSITIONS

Consider a three-level bare-state atomic system with two upper levels $|a\rangle$ and $|b\rangle$ and one ground level $|g\rangle$ (see Fig. 1). We assume that the two upper bare levels have opposite parity, and that the parity of the ground level is even. For example, level $|b\rangle$ possesses an even parity while level $|a\rangle$ has an odd parity. In general, such an atomic system can be found in alkali-metal atoms. Note that the $|a\rangle$-$|b\rangle$ transition [energy separation $\hbar\omega_{ab}=\hbar(\omega_a-\omega_b)$] can be driven by a strong-coupling laser beam (radian frequency ω_c). Let us first consider the dressed states that contain the information on the interaction between the two-level system levels $\{|a\rangle,|b\rangle\}$ and the strong-coupling field. The undisturbed Hamiltonian is

$$H_0=\begin{bmatrix}\hbar\omega_a & 0\\ 0 & \hbar\omega_b\end{bmatrix} \tag{1}$$

which is disturbed by H_1

$$H_1=\begin{bmatrix}0 & -\wp_{ab}E_c(t)\\ -\wp_{ba}E_c(t) & 0\end{bmatrix}, \tag{2a}$$

$$E_c(t)=\mathcal{E}_c\cos(\omega_c t). \tag{2b}$$

Transformation to the interaction picture involves the unitary matrix $U_0=e^{-iH_0t/\hbar}$ taking the Schrödinger picture operator O_S to $O_I(t)=U_0^\dagger(t)O_SU_0(t)$, and in this picture H_0 is unchanged but H_1 becomes

$$H_{I1}=-\frac{1}{2}\begin{bmatrix}0 & -\wp_{ab}(e^{i(\omega_{ab}+\omega_c)t}+e^{i\delta t})\\ -\wp_{ba}(e^{-i(\omega_{ab}+\omega_c)t}+e^{-i\delta t}) & 0\end{bmatrix}. \tag{3}$$

Dropping the $e^{\pm i(\omega_{ab}+\omega_c)}$ terms in the rotating wave approximation (RWA) because they are so rapidly varying, we have

$$H_{I1}=-\frac{\hbar\Omega_R}{2}\begin{bmatrix}0 & e^{i\phi}e^{i\delta t}\\ e^{-i\phi}e^{-i\delta t} & 0\end{bmatrix},$$

$$\Omega_R=\frac{|\wp_{ab}|\mathcal{E}_c}{\hbar},\quad \wp_{ab}=|\wp_{ab}|e^{i\phi_c}, \tag{4}$$

where $\delta=\omega_{ab}-\omega_c$ is the frequency detuning of the coupling field. This may also be written in terms of the complex Rabi coupling frequency $\Omega_{Rc}=\Omega_Re^{i\phi_c}$ in the compact form in the nearly on-resonance condition ($\delta\approx 0$),

$$H_{I1}=\begin{bmatrix}0 & V\\ V^* & 0\end{bmatrix},\quad V=\hbar\Omega_Re^{i\phi}/2,\quad \phi=\phi_c+(2n-1)\pi. \tag{5}$$

Here the spontaneous decay effect in the bare-state system $\{|a\rangle,|b\rangle\}$ can be neglected if the intensity of the applied coupling field E_c is very strong (i.e., $|V|\gg\hbar\Gamma$, with Γ being the spontaneous emission decay rate).

The dressed-state system is obtained by working in the equations of motion wave function system of equations in the original system and then transforming to a new basis set for the diagonalized matrix of that system,

$$|\psi_S(\mathbf{r},t)\rangle=C_a(t)e^{i(\delta/2-\omega_a)t}|a\rangle+C_b(t)e^{i(-\delta/2-\omega_b)t}|b\rangle. \tag{6}$$

The interaction picture wave function is then $|\psi_I(\mathbf{r},t)\rangle=U_0^\dagger(t)|\psi_S(\mathbf{r},t)\rangle$,

$$|\psi_I(\mathbf{r},t)\rangle=C_a(t)e^{i\delta t/2}|a\rangle+C_b(t)e^{-i\delta t/2}|b\rangle, \tag{7}$$

which obeys the interaction wave equation

$$\frac{\partial}{\partial t}|\psi_I(t)\rangle=-\frac{i}{\hbar}H_{I1}|\psi_I(t)\rangle. \tag{8}$$

Inserting (4) for H_{I1} and (7) for $|\psi_I(\mathbf{r},t)\rangle$, one finds that

$$\frac{d}{dt}\begin{bmatrix}C_a(t)\\ C_b(t)\end{bmatrix}=\frac{i}{\hbar}\begin{bmatrix}\hbar\delta/2 & -\hbar\Omega_{Rc}/2\\ -\hbar\Omega_{Rc}^*/2 & -\hbar\delta/2\end{bmatrix}\begin{bmatrix}C_a(t)\\ C_b(t)\end{bmatrix} \tag{9}$$

for the equation of motion (EoM) of the wave function coefficients, after having used a judicious choice of time variation in (6) with an explicit half-detuning period. From (5) we realize that this EoM may be recast as

$$\frac{d}{dt}\begin{bmatrix}C_a(t)\\ C_b(t)\end{bmatrix}=\frac{i}{\hbar}H_{\text{equ}}^{\text{EoM}}\begin{bmatrix}C_a(t)\\ C_b(t)\end{bmatrix},\quad H_{\text{equ}}^{\text{EoM}}=\begin{bmatrix}\hbar\delta/2 & V\\ V^* & -\hbar\delta/2\end{bmatrix}, \tag{10}$$

where $H_{\text{equ}}^{\text{EoM}}$ is the equivalent Hamiltonian for the equation of motion.

The equivalent Hamiltonian, the EoM matrix, is diagonalized by using a unitary matrix U_d, forming $H_{\text{Dequ}}^{\text{EoM}}=U_d^{-1}H_{\text{equ}}^{\text{EoM}}U_d$, where U_d is found as the columns made up of the system eigenvectors of $H_{\text{equ}}^{\text{EoM}}$ [27],

$$U_d=\left[\begin{pmatrix}\alpha_+\\ \beta_+\end{pmatrix}\begin{pmatrix}\alpha_-\\ \beta_-\end{pmatrix}\right]=\left[\begin{pmatrix}\cos\vartheta\\ e^{-i\phi}\sin\vartheta\end{pmatrix}\begin{pmatrix}-\sin\vartheta\\ e^{-i\phi}\cos\vartheta\end{pmatrix}\right] \tag{11}$$

with the dressed wave function coefficients being expressible as

$$\begin{bmatrix} C_+(t) \\ C_-(t) \end{bmatrix} = U \begin{bmatrix} C_a(t) \\ C_b(t) \end{bmatrix}, \quad U = U_d^{-1} = U_d^{\dagger}, \tag{12}$$

which can be restated as [28,29]

$$|+\rangle = \cos\vartheta|a\rangle + e^{i\phi}\sin\vartheta|b\rangle,$$

$$|-\rangle = -\sin\vartheta|a\rangle + e^{i\phi}\cos\vartheta|b\rangle, \tag{13}$$

where

$$\cos\vartheta = \frac{1}{\sqrt{2}}\left[1 - \frac{1}{\sqrt{1+4\dfrac{|\Omega_{Rc}|^2}{\delta^2}}}\right]^{1/2},$$

$$\sin\vartheta = \frac{1}{\sqrt{2}}\left[1 + \frac{1}{\sqrt{1+4\dfrac{|\Omega_{Rc}|^2}{\delta^2}}}\right]^{1/2}. \tag{14}$$

Choice of signs for both radicals is based upon agreement with the solution for the $\phi=0$ case available in [30] and for the 2ϑ cosinusoidal expressions. The derivation of (14) and the $\phi=0$ case are provided in Appendices A and B.

Mid-energy between states $|a\rangle$ and $|b\rangle$ is $\hbar\bar{\omega}$, where $\bar{\omega}=(\omega_a+\omega_b)/2$, and because $\omega_{a,b}=\bar{\omega}\pm\omega_{ab}/2$, one can write $\omega_a=\bar{\omega}+(\omega_c+\delta)/2$ and $\omega_a=\bar{\omega}-(\omega_c+\delta)/2$, utilizing the detuning δ. Adding the Hamiltonian parts H_{I0} and H_{I1} from (1) and (5) yields the total interaction Hamiltonian,

$$H_{I1} = \begin{bmatrix} \hbar\omega_a & V \\ V^* & \hbar\omega_b \end{bmatrix}, \tag{15}$$

whose eigenvalues are the new energies of the highly driven two-level system $\{|a\rangle,|b\rangle\}$,

$$\omega_{\pm} = \bar{\omega} \pm \frac{1}{2}\sqrt{\omega_{ab}{}^2 + |\Omega_{Rc}|^2} \tag{16}$$

with a separation change from ω_{ab} to $\omega_{+-}=\sqrt{\omega_{ab}{}^2+|\Omega_{Rc}|^2}$.

Bare states have pure parities, whereas the dressed states have mixed parities. Thus, both the electric and magnetic fields of a weak probe field (with mode frequency ω_p; the Rabi frequency of the probe field Ω_p, discussed below, satisfies $\Omega_p \ll < \gamma_-, \gamma_g$) can drive a transition between a third state, referred to as the ground state $|g\rangle$, and either of the bare states $|a\rangle$ and $|b\rangle$, which under intense coupling field light can be viewed as a dressed-state pair $\{|+\rangle, |-\rangle\}$. Because under many conditions, certainly under quasiequilibrium conditions where a Boltzmann distribution of state occupation may apply, or even under driven conditions when the energy level separation decreases the occupation number of a removed upper level, we will assume our probe field causes transitions between the ground state and lower dressed state $|-\rangle$, and we will ignore in modeling the upper dressed state $|+\rangle$. The interaction Hamiltonian of the $\{|-\rangle, |g\rangle\}$ pair is

$$H_1 = \begin{bmatrix} -\wp_{--}E_p(t) & -\wp_{-g}E_p(t) \\ -\wp_{g-}E_p(t) & -\wp_{gg}E_p(t) \end{bmatrix} + \begin{bmatrix} -\mathscr{m}_{--}B_p(t) & -\mathscr{m}_{-g}B_p(t) \\ -\mathscr{m}_{g-}B_p(t) & -\mathscr{m}_{gg}B_p(t) \end{bmatrix}, \quad B_p(t) = \mathcal{B}_p\cos(\omega_p t), \tag{17}$$

where the various matrix off-diagonal elements of the $\{|+\rangle,|-\rangle\}$ fully dressed and hybrid $\{|-\rangle,|g\rangle\}$ systems are

$$\begin{aligned}\wp_{+-} &= \langle + |\mathbf{D}_e| - \rangle \\ &= (\cos\vartheta\langle a| + e^{-i\phi}\sin\vartheta\langle b|)\mathbf{D}_e(-\sin\vartheta|a\rangle + e^{i\phi}\cos\vartheta|b\rangle) \\ &= \wp_{ab}e^{i\phi}\cos^2\vartheta - \wp_{ba}e^{-i\phi}\sin^2\vartheta,\end{aligned}$$

$$\begin{aligned}\mathscr{m}_{+-} &= \langle + |\mathbf{D}_m| - \rangle \\ &= (\cos\vartheta\langle a| + e^{-i\phi}\sin\vartheta\langle b|)\mathbf{D}_m(-\sin\vartheta|a\rangle + e^{i\phi}\cos\vartheta|b\rangle) \\ &= (\mathscr{m}_{bb} - \mathscr{m}_{aa})\cos\vartheta\sin\vartheta,\end{aligned} \tag{18}$$

$$\begin{aligned}\wp_{-g} &= \langle - |\mathbf{D}_e| g \rangle \\ &= (-\sin\vartheta\langle a| + e^{-i\phi}\cos\vartheta\langle b|)\mathbf{D}_e|g\rangle \\ &= -\wp_{ag}\sin\vartheta,\end{aligned}$$

$$\begin{aligned}\mathscr{m}_{-g} &= \langle - |\mathbf{D}_m| g \rangle \\ &= (-\sin\vartheta\langle a| + e^{-i\phi}\cos\vartheta\langle b|)\mathbf{D}_m|g\rangle \\ &= \mathscr{m}_{bg}e^{-i\phi}\cos\vartheta.\end{aligned} \tag{19}$$

Evolution of the states can be conveniently described by a density matrix ρ formulation employing the phenomenological Liouville equation. The equation of motion is

$$\frac{\partial\rho}{\partial t} = -\frac{i}{\hbar}[H, \rho] - \frac{1}{2}\{\Gamma, \rho\}, \tag{20}$$

and following [31] for a diagonal Γ operator, namely, $\langle n|\Gamma|m\rangle = \gamma_n\delta_{nm}$, we obtain

$$\Gamma = \begin{bmatrix} \gamma_- & 0 \\ 0 & \gamma_g \end{bmatrix}. \tag{21}$$

Diagonal and off-diagonal equations of motion for ρ are

$$\frac{\partial\rho_{--}}{\partial t} = \frac{i}{\hbar}[\wp_{-g}E(t) + \mathscr{m}_{-g}B(t)]\rho_{g-} + \text{c.c.} - \gamma_-\rho_{--},$$

$$\frac{\partial\rho_{gg}}{\partial t} = \frac{i}{\hbar}[\wp_{g-}E(t) + \mathscr{m}_{g-}B(t)]\rho_{-g} + \text{c.c.} - \gamma_g\rho_{gg},$$

$$\begin{aligned}\frac{\partial\rho_{-g}}{\partial t} = &\left(i\omega_{-g} + \frac{i}{\hbar}(\wp_{gg} - \wp_{--})E(t) + \frac{i}{\hbar}(\mathscr{m}_{gg} - \mathscr{m}_{--})B(t)\right)\rho_{-g} \\ &- \frac{i}{\hbar}[\wp_{-g}E(t) + \mathscr{m}_{-g}B(t)](\rho_{--} - \rho_{gg}) - \frac{1}{2}(\gamma_- + \gamma_g)\rho_{-g}.\end{aligned} \tag{22}$$

where c.c. is the complex conjugate.

On a microscopic level, a probe field traveling through the medium has

$$E_p(t) = E_{px}(t) = \mathcal{E}_p \cos(\omega_p t),$$

$$B_p(t) = B_{py}(t) = \mathcal{B}_p \cos(\omega_p t), \quad \mathcal{B}_p/\mathcal{E}_p = k/\omega_p, \tag{23}$$

which, when inserted into the density matrix equations of motion (22), enlisting

$$\rho_{-g}(t) = \tilde{\rho}_{-g}(t) e^{-i\omega_p t}, \tag{24}$$

yields in the rotating wave approximation

$$\frac{\partial \rho_{--}}{\partial t} = \frac{i}{2}(\Omega_p \tilde{\rho}_{g-} - \Omega_p{}^* \tilde{\rho}_{-g}) - \gamma_- \rho_{--},$$

$$\frac{\partial \rho_{gg}}{\partial t} = \frac{i}{2}(\Omega_p{}^* \tilde{\rho}_{-g} - \Omega_p \tilde{\rho}_{g-}) - \gamma_g \rho_{gg},$$

$$\frac{\partial \tilde{\rho}_{-g}}{\partial t} = \frac{i}{2}\Omega_p(\rho_{gg} - \rho_{--}) - \left(\frac{\gamma_- + \gamma_g}{2} + i\Delta\right)\tilde{\rho}_{-g}, \tag{25}$$

where the probe electric, magnetic, and total Rabi frequencies are defined as

$$\Omega_p^E = \frac{\wp_{-g}\mathcal{E}_p}{\hbar}, \quad \Omega_p^B = \frac{\mathfrak{m}_{-g}\mathcal{B}_p}{\hbar}, \quad \Omega_p = \Omega_p^E + \Omega_p^B. \tag{26}$$

Frequency detuning of the weak probe light is defined as $\Delta = \omega_{-g} - \omega_p$ (with ω_{-g} being the frequency separation of the $|-\rangle$-$|g\rangle$ transition). In the steady state the off-diagonal element of the density matrix obeys

$$\frac{\partial \tilde{\rho}_{-g}}{\partial t} = 0, \tag{27}$$

and applying this for (25) gives

$$\tilde{\rho}_{-g} = \frac{\Omega_p}{2}\left(\frac{\Delta + i(\gamma_- + \gamma_g)/2}{\Delta^2 + [(\gamma_- + \gamma_g)/2]^2}\right)(\rho_{gg} - \rho_{--}), \tag{28}$$

which, in the limit of no decay from the ground level ($\gamma_g = 0$) and assuming we started out with the population of states in $|g\rangle$ nearly full, and the thermal excitation to level $|-\rangle$ negligible, we set $\rho_{gg} \approx 1$ and $\rho_{--} \approx 0$, reducing (28) to

$$\tilde{\rho}_{-g} = \frac{\Omega_p}{2}\left(\frac{\Delta + i\gamma_-/2}{\Delta^2 + (\gamma_-/2)^2}\right). \tag{29}$$

In the next section, we give expressions for the atomic (electric) polarizability and (magnetic) magnetizability of the transition excited by the weak probe field. The electric permittivity and the magnetic permeability as well as the refractive index of the atomic vapor can then be derived.

III. EFFECT OF QUANTIZING THE PROBE BEAM

The most general total Hamiltonian expression H, using a Jaynes-Cumming approach, in the Schrödinger picture for the system with quantized photon field is

$$H = H_{0L} + H_1^{\mathrm{em}} + H^{\mathrm{ph}}, \tag{30}$$

with

$$H_{0L} = \hbar(\omega_- - \omega_g)\sigma_z/2,$$

$$H_1^{\mathrm{em}} = \begin{bmatrix} -\wp_{--}E_p^Q(t) & -\wp_{-g}E_p^Q(t) \\ -\wp_{g-}E_p^Q(t) & -\wp_{gg}E_p^Q(t) \end{bmatrix} + \begin{bmatrix} -\mathfrak{m}_{--}B_p^Q(t) & -\mathfrak{m}_{-g}B_p^Q(t) \\ -\mathfrak{m}_{g-}B_p^Q(t) & -\mathfrak{m}_{gg}B_p^Q(t) \end{bmatrix}$$

$$H^{\mathrm{ph}} = \hbar(a^\dagger a + 1/2)\omega_p, \tag{31}$$

where the H_{0L} form is for symmetrization about $H_{0L}=0$ using the Pauli operator. Form (1) works just as well. Equation (31) for H_1^{em} using the quantized electric $E_p^Q(t)$ and magnetic $B_p^Q(t)$ fields is identical in form to (17), with the traveling wave nature of the photons in (23) (subtract kz from $\omega_p t$ to see the explicit wave propagation in the $+z$ direction; the earlier field was examined at $z=0$) represented by the second-quantization operators $a=a(t)$ and $a^\dagger = a^\dagger(t)$. Thus $E_p^Q(t) = \mathcal{E}_{\omega_p}(a+a^\dagger)/\sqrt{2}$ and $B_p^Q(t) = \mathcal{B}_{\omega_p}(a+a^\dagger)/\sqrt{2}$ with $\mathcal{E}_{\omega_p} = \sqrt{\hbar\omega_p/\varepsilon_0 V}$ and $\mathcal{B}_{\omega_p} = \sqrt{\hbar\omega_p\mu_0/V}$, where V is a characteristic interaction volume. For a standing wave pattern in a cavity, V is the cavity volume, and $E_p^Q(t)$ and $B_p^Q(t)$ change to $E_p^Q(t) = \mathcal{E}_{\omega_p}(a+a^\dagger)\sin kz$ and $B_p^Q(t) = -i\mathcal{B}_{\omega_p}(a-a^\dagger)\cos kz$.

The equations of motion in (25) become in the manifold of the $|-n\rangle$-$|g(n+1)\rangle$ states

$$\frac{\partial \rho_{-n;-n}}{\partial t} = \frac{i}{2}(\Omega_p^Q \tilde{\rho}_{g(n+1);-n} - \Omega_p^{Q*} \tilde{\rho}_{-ng(n+1)}) - \gamma_{-n}\rho_{-n;-n},$$

$$\frac{\partial \rho_{g(n+1);g(n+1)}}{\partial t} = \frac{i}{2}(\Omega_p^{Q*} \tilde{\rho}_{-g} - \Omega_p^Q \tilde{\rho}_{g(n+1);-n}) - \gamma_{g(n+1)}\rho_{g(n+1);g(n+1)},$$

$$\frac{\partial \tilde{\rho}_{-n;g(n+1)}}{\partial t} = \frac{i}{2}\Omega_p^Q(\rho_{g(n+1);g(n+1)} - \rho_{-n;-n}) - \left(\frac{\gamma_{-n} + \gamma_{g(n+1)}}{2} + i\Delta_n\right)\tilde{\rho}_{-n;g(n+1)}, \tag{32}$$

where the probe electric, magnetic, and total Rabi frequencies are now defined as

$$\Omega_p^{QE} = \frac{\wp_{-g}\mathcal{E}_{\omega_p}\sqrt{2(n+1)}}{\hbar}, \quad \Omega_p^{QB} = \frac{\mathfrak{m}_{-g}\mathcal{B}_{\omega_p}\sqrt{2(n+1)}}{\hbar\sqrt{2}},$$

$$\Omega_p^Q = \Omega_p^{QE} + \Omega_p^{QB}, \tag{33}$$

and the frequency detuning of the weak probe light is defined as $\Delta_n = \omega_{-n;g(n+1)} - \omega_p$ (with $\omega_{-n;g(n+1)}$ being the frequency separation of the $|-n\rangle$-$|g(n+1)\rangle$ transition). (Note that the decay constants and bare-state level separation were upgraded to appear consistent with the manifold notation—strictly speaking all of this could be done in the dressed-state space of the $|-n\rangle$-$|g(n+1)\rangle$ manifold—see Appendix C.) Use of a cavity model for the photonic field will alter Ω_p^Q to become $\Omega_p^Q = \Omega_p^{QE} - i\Omega_p^{QB}$. In the steady state the off-diagonal element of the density matrix obeys

$$\frac{\partial \tilde{\rho}_{-n;g(n+1)}}{\partial t} = 0, \tag{34}$$

and applying this to (32) gives

$$\tilde{\rho}_{-n;g(n+1)} = \frac{\Omega_p^Q}{2}\left(\frac{\Delta_n + i(\gamma_{-n} + \gamma_{g(n+1)})/2}{\Delta_n{}^2 + [(\gamma_{-n} + \gamma_{g(n+1)})/2]^2}\right) \times (\rho_{g(n+1);g(n+1)} - \rho_{-n;-n}). \tag{35}$$

In the limit of no decay from the ground level of the atomic-photonic state ($\gamma_{g(n+1)}=0$), assuming we started out with the population of states in $|g(n+1)\rangle$ nearly full and the thermal excitation to level $|-n\rangle$ negligible, setting $\rho_{g(n+1);g(n+1)} \approx 1$ and $\rho_{-n;-n} \approx 0$, (35) is reduced to

$$\tilde{\rho}_{-g} = \frac{\Omega_p^Q}{2}\left(\frac{\Delta_n + i\gamma_-/2}{\Delta_n{}^2 + (\gamma_-/2)^2}\right). \tag{36}$$

Association of a photon number n with a classical intensity of our probe beam can be accomplished by equating the Rabi frequencies for the semiclassical approach found in (26) and for the fully quantum mechanical approach found in (33). That is, setting

$$\Omega_p^{QE} = \Omega_p^E, \quad \Omega_p^{QB} = \Omega_p^B \tag{37}$$

yields

$$n + 1 = \frac{\varepsilon_0 V}{2\hbar\omega_p}\mathcal{E}_p{}^2, \tag{38}$$

which in the case of large photon numbers, probably the case except in all but a few photon events, transforms into

$$n = \frac{\varepsilon_0 V}{2\hbar\omega_p}\mathcal{E}_p{}^2. \tag{38$'$}$$

The energy eigenvalues, expressed in radian frequencies, may be compactly written as

$$\omega_{-n,g(n+1)} = (n+1)\omega_p \pm \sqrt{(\Delta_n/2)^2 + \Omega_p^{Q^2}/4}, \tag{39}$$

as discussed in Appendix C.

IV. ATOMIC POLARIZABITY AND MAGNETIZABILITY AND DETERMINATION OF THE PERMITTIVITY AND PERMEABILITY

The atomic electric polarizability α_e due to the $|-\rangle$-$|g\rangle$ transition can be found by obtaining the quantum mechanical $\mathbf{P}^{\mathrm{QM}}$ and electromagnetic $\mathbf{P}^{\mathrm{EM}}$ polarizations, equating them, and extracting out the electric polarizability. Following a similar argument found in a two-species two-level system [32], $\mathbf{P}^{\mathrm{EM}}$ is given by

$$\mathbf{P}^{\mathrm{QM}} = \langle\psi|\mathbf{D}_e|\psi\rangle = \mathrm{Tr}\{\rho\wp\} = \sum_p \sum_q \rho_{pq}\wp_{qp}, \quad \mathbf{D}_e = e\mathbf{r}, \tag{40}$$

where the electron charge has a minus sign in it. Electromagnetic representation $\mathbf{P}^{\mathrm{EM}}$ is given by

$$\mathbf{P}^{\mathrm{EM}} = \mathbf{P}(t)e^{-i\omega t} + \text{c.c.} \tag{41}$$

Equating the two representations for the simple model we are treating here with single field components, we obtain

$$P^{\mathrm{QM}} = P^{\mathrm{EM}}, \tag{42}$$

or

$$\rho_{--}\wp_{--} + \tilde{\rho}_{-g}e^{-i\omega t}\wp_{-g} + \tilde{\rho}_{g-}e^{i\omega t}\wp_{g-} + \rho_{gg}\wp_{gg} = \mathcal{P}(t)e^{-i\omega t} + \mathcal{P}^*(t)e^{i\omega t} \tag{43}$$

using (24). Recognizing that (43) contains two copies of the same fundamental equation, after employing the RWA, we obtain

$$\mathcal{P}(t) = \tilde{\rho}_{-g}\wp_{g-}, \tag{44}$$

which, when the slowing varying density matrix off-diagonal element given in (28) is inserted, results in

$$\mathcal{P}(t) = \frac{1}{2}\left(\frac{\wp_{-g}\wp_{g-}}{\hbar}\mathcal{E}_p + \frac{\mathscr{m}_{-g}\wp_{g-}}{\hbar}\mathcal{B}_p\right)\left(\frac{\Delta + i(\gamma_- + \gamma_g)/2}{\Delta^2 + [(\gamma_- + \gamma_g)/2]^2}\right) \times (\rho_{gg} - \rho_{--}). \tag{45}$$

Applying the approximations we used before to obtain (29) reduces (45) to

$$\mathcal{P} = \frac{1}{2}\left(\frac{\wp_{-g}\wp_{g-}}{\hbar}\mathcal{E}_p + \frac{\mathscr{m}_{-g}\wp_{g-}}{\hbar}\mathcal{B}_p\right)\left(\frac{\Delta + i\gamma_-/2}{\Delta^2 + (\gamma_-/2)^2}\right), \tag{46}$$

where we have dropped the explicit time dependence since it falls out. The atomic electric polarizability α_e can now be found, noting that in the frequency domain $\mathcal{P}(\omega)$ is related to the local electric microscopic field $\mathcal{E}_p$ by

$$\mathcal{P}(\omega) = \varepsilon_0\alpha_e\mathcal{E}_p. \tag{47}$$

Using $\mathcal{B}_p/\mathcal{E}_p = k/\omega_p$ from (23), or

$$\mathcal{B}_p/\mathcal{E}_p = \sqrt{\mu_0\varepsilon_0} \tag{48}$$

where (48) has an implicit assumption about the local fields around the atom versus the externally applied probe field, we obtain

$$\alpha_e = \frac{1}{2}\frac{\Delta + i\gamma_-/2}{\hbar[\Delta^2 + (\gamma_-/2)^2]}\left(\frac{\wp_{-g}\wp_{g-}}{\varepsilon_0} + \sqrt{\frac{\mu_0}{\varepsilon_0}}\mathscr{m}_{-g}\wp_{g-}\right). \tag{49}$$

The atomic magnetizability α_m due to the $|-\rangle$-$|g\rangle$ transition can be found by obtaining the quantum mechanical $\mathbf{M}^{\mathrm{QM}}$ and electromagnetic $\mathbf{M}^{\mathrm{EM}}$ magnetizations, equating them, and extracting out the magnetizability. $\mathbf{M}^{\mathrm{EM}}$ is given by [32]

$$\mathbf{M}^{\mathrm{QM}} = \langle\psi|\mathbf{D}_m|\psi\rangle = \mathrm{Tr}\{\rho\mathscr{m}\} = \sum_p \sum_q \rho_{pq}\mathscr{m}_{qp},$$

$$\mathbf{D}_m = (e/2m)(\mathbf{L} + 2\mathbf{S}). \tag{50}$$

Electromagnetic representation $\mathbf{M}^{\mathrm{EM}}$ is given by

$$M^{\mathrm{EM}} = \mathcal{M}(t)e^{-i\omega t} + \text{c.c.} \tag{51}$$

Equating the two representations for the simple model we are treating here with single field components, we obtain

$$M^{\mathrm{QM}} = M^{\mathrm{EM}} \tag{52}$$

or

$$\rho_{--}m_{--} + \tilde{\rho}_{-g}e^{-i\omega t}m_{-g} + \tilde{\rho}_{g-}e^{i\omega t}m_{g-} + \rho_{gg}m_{gg} = \mathcal{M}(t)e^{-i\omega t} + \mathcal{M}^*(t)e^{i\omega t} \tag{53}$$

using (24). Recognizing that (53) contains two copies of the same fundamental equation, after employing the RWA, we obtain

$$\mathcal{M}(t) = \tilde{\rho}_{-g}m_{g-}, \tag{54}$$

which, when the slowing varying density matrix off-diagonal element given in (28) is inserted, results in

$$\mathcal{M}(t) = \frac{1}{2}\left(\frac{p_{-g}m_{g-}}{\hbar}\mathcal{E}_p + \frac{m_{-g}m_{g-}}{\hbar}\mathcal{B}_p\right)\left(\frac{\Delta + i(\gamma_- + \gamma_g)/2}{\Delta^2 + [(\gamma_- + \gamma_g)/2]^2}\right) \times(\rho_{gg} - \rho_{--}). \tag{55}$$

Application of the approximations we used before to obtain (29) reduces (55) to

$$\mathcal{M} = \frac{1}{2}\left(\frac{p_{-g}m_{g-}}{\hbar}\mathcal{E}_p + \frac{m_{-g}m_{g-}}{\hbar}\mathcal{B}_p\right)\left(\frac{\Delta + i\gamma_-/2}{\Delta^2 + (\gamma_-/2)^2}\right), \tag{56}$$

where we have dropped the explicit time dependence since it falls out. Here the atomic magnetizability α_m can now be found, noting that in the frequency domain $\mathcal{M}(\omega)$ is related to the local electric microscopic field $\mathcal{B}_p$ by

$$\mathcal{M}(\omega) = \alpha_m \mathcal{B}_p/\mu_0. \tag{57}$$

Using (46), we obtain

$$\alpha_m = \frac{1}{2}\frac{\Delta + i\gamma_-/2}{\hbar[\Delta^2 + (\gamma_-/2)^2]}\left(\sqrt{\frac{\mu_0}{\varepsilon_0}}p_{-g}m_{g-} + \mu_0 m_{-g}m_{g-}\right). \tag{58}$$

Macroscopic electric and magnetic susceptibilities, and consequently the permittivity and permeability of the vapor medium, may be found from the atom polarizability and magnetizability. Electric susceptability is found by employing (47), using the Clausius-Mossotti relation, which takes account of the local field effect due to the electric dipole-dipole interaction between neighboring atoms:

$$\chi_e = \frac{N\alpha_e}{1 - N\alpha_e/3}, \tag{59}$$

making the relative permittivity

$$\varepsilon_r = \varepsilon_{br} + \chi_e = 1 + \chi_e = 1 + \frac{N\alpha_e}{1 - N\alpha_e/3}, \tag{60}$$

where the second equality holds in a low-density gas, but not for a solid medium. Magnetic susceptibility is found by employing (58), again using a Clausius-Mossotti relation, which takes account of the local field effect due to the magnetic dipole-dipole interaction between neighboring atoms

$$\chi_m = \frac{N\alpha_m}{1 - N\alpha_m/3}, \tag{61}$$

making the permeability

$$\mu_r = \frac{\mu_{br}}{1 - \chi_m} = \frac{1}{1 - \chi_m}, \tag{62}$$

where the last equality holds in a low-density gas, but not for a solid medium. Inserting (61) into (62) yields

$$\mu_r = 1 + \frac{N\alpha_m}{1 - 4N\alpha_m/3}, \tag{63}$$

which is similar in form to the last expression in (60) for the permittivity.

It is readily seen, invoking the field equivalency to the photon count n using (37), that in the manifold of the $|-n\rangle$-$|g(n+1)\rangle$ states, α_e and α_m are in identical forms to (49) and (58). That is,

$$\alpha_e = \frac{1}{2}\frac{\Delta_n + i\gamma_{-n}/2}{\hbar[\Delta_n^2 + (\gamma_{-n}/2)^2]}\left(\frac{p_{-g}p_{g-}}{\varepsilon_0} + \sqrt{\frac{\mu_0}{\varepsilon_0}}m_{-g}p_{g-}\right), \tag{64}$$

$$\alpha_m = \frac{1}{2}\frac{\Delta_n + i\gamma_{-n}/2}{\hbar[\Delta_n^2 + (\gamma_{-n}/2)^2]}\left(\sqrt{\frac{\mu_0}{\varepsilon_0}}p_{-g}m_{g-} + \mu_0 m_{-g}m_{g-}\right). \tag{65}$$

V. NEGATIVE REFRACTIVE INDEX

Before converting the permittivity and permeability into refractive index n, one must address the issue of taking the appropriate branch. These formulas will be obtained, and then utilized to look at a typical example numerically to show that such a scheme can exhibit a negative refractive index. The formula adopted is

$$n_r = \sqrt{\mu_r}\sqrt{\varepsilon_r} \tag{66}$$

rather than $n_r = \sqrt{\mu_r\varepsilon_r}$, and we have verified that (66) is valid for either left- or right-handed media in which $\mathrm{Re}(\mu_r) < 0$ and $\mathrm{Re}(\varepsilon_r) < 0$ or $\mathrm{Re}(\mu_r) > 0$ and $\mathrm{Re}(\varepsilon_r) > 0$ for passive lossy cases $[\mathrm{Im}(\mu_r) > 0$ and $\mathrm{Im}(\varepsilon_r) > 0]$. Writing

$$\varepsilon_r = -A + Bi, \quad u_r = -C + Di, \tag{67}$$

where our passive left-handed medium has $A > 0$, $B > 0$ and $C > 0$, $D > 0$, the square roots can be then expressed as

$$\sqrt{\varepsilon_r} = i(a + bi), \quad \sqrt{u_r} = i(c + di). \tag{68}$$

Parameters a, b, c, and d can be solved from quadratic equations as

$$a = \pm\sqrt{\frac{\pm\sqrt{A^2 + B^2} + A}{2}}, \quad b = \mp\sqrt{\frac{\pm\sqrt{A^2 + B^2} - A}{2}}, \tag{69}$$

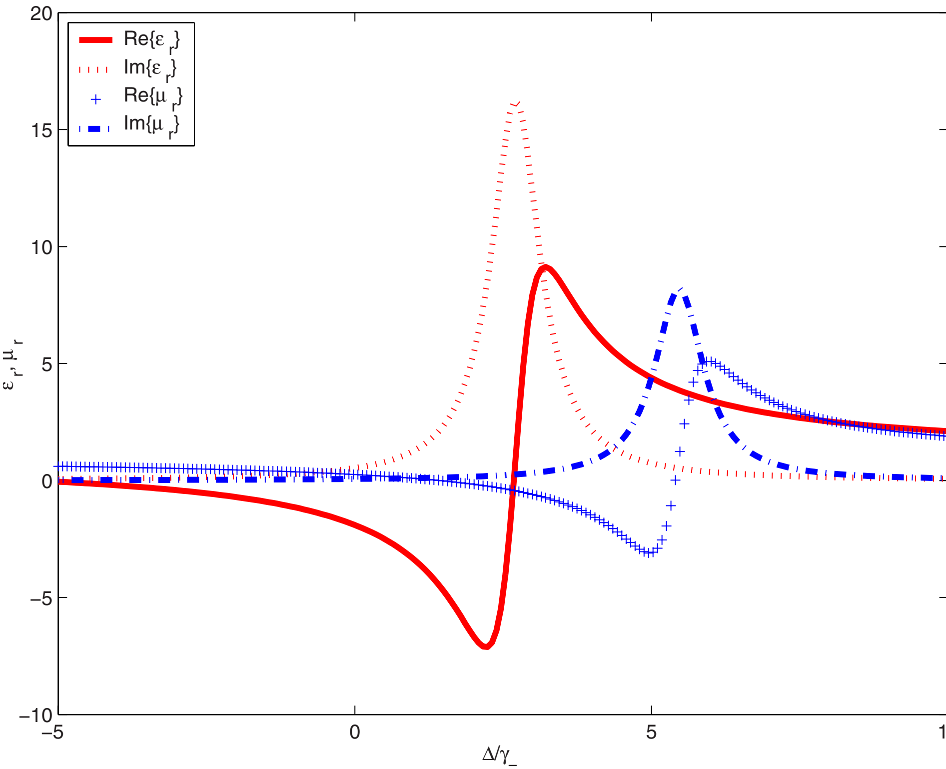

FIG. 2. (Color online) Dispersion behavior of the real and imaginary parts of the relative permittivity ε_r and permeability μ_r, versus normalized detuning frequency Δ/γ_-, in the dressed-state mixed-parity medium.

$$c = \pm\sqrt{\frac{\pm\sqrt{C^2+D^2}+C}{2}}, \quad d = \mp\sqrt{\frac{\pm\sqrt{C^2+D^2}-C}{2}}. \tag{70}$$

Only the plus sign under the inner radical must be used to assure that the parameters a, b, c, and d are real. Next, the outer radical signs must be selected as either $+$, $+$ for a and c or $-$, $-$ to assure that for a poynting vector propagating, say, in the $+z$ direction, the field variation $\exp\{i[\omega\,\mathrm{Re}(n_r)z/c-\omega t]\}\ \exp[-\omega\,\mathrm{Im}(n_r)z/c]$ has the proper backward or forward phase propagation behavior and decay for a passive medium. With these thoughts in mind, the parameters may be set down as

$$a = \sqrt{\frac{\sqrt{A^2+B^2}+A}{2}}, \quad b = -\sqrt{\frac{\sqrt{A^2+B^2}-A}{2}}, \tag{71}$$

$$c = \sqrt{\frac{\sqrt{C^2+D^2}+C}{2}}, \quad d = -\sqrt{\frac{\sqrt{C^2+D^2}-C}{2}}. \tag{72}$$

The refractive index of the atomic vapor due to the mixed-parity transitions in the hybrid system is given by

$$n_r = -[(ac-bd)+(ad+bc)i]. \tag{73}$$

It then follows for a left-handed medium that $ac-bd>0$ and $ad+bc<0$, and n_r has a negative real part and a positive imaginary part. On the other hand, if the medium is right handed with ε_r and μ_r having positive real parts, i.e., $A<0$, $C<0$, then $ac-bd<0$ and $ad+bc<0$, and both the real and imaginary parts of n_r are positive.

VI. NUMERICAL EXAMPLE

Using the analysis of the previous sections, the dispersive behavior of the relative permittivity ε_r and permeability μ_r (Fig. 2) and the refractive index n_r of the atomic vapor, can be computed and plotted (Fig. 3). Typical values for the parameters of the atomic system are chosen to be $\wp_{ag}=4.00\times10^{-29}$ C m, $\mathscr{m}_{bg}=8.76\times10^{-23}$ C m^2 s^{-1}, coupling frequency detuning $\delta=4.0\times10^9$ s^{-1}, and Rabi coupling frequency $\Omega_{\mathcal{R}}=|\wp_{ab}|\mathcal{E}_c/\hbar=5.8\times10^7$ s^{-1}. According to (19), the magnitudes of $\wp_{-g}$ and $\mathscr{m}_{-g}$ are, respectively, $\wp_{-g}=5.80\times10^{-31}$ C m and $\mathscr{m}_{-g}=8.76\times10^{-23}$ C m^2 s^{-1}. [For simplicity, $\phi=0$ at this stage—see (19).] The decay rate γ_- (including the effects of spontaneous emission and nonradiative collisional dephasing) and atomic concentration N are, respectively, $\gamma_-=1.0\times10^7$ s^{-1} and $N=3.0\times10^{23}$ m^{-3}. Figure 2 shows that the negative swing of $\mathrm{Re}(\varepsilon_r)$ is much larger than that of $\mathrm{Re}(\mu_r)$, not an entirely surprising result, recognizing the historical difficulty of obtaining negativity in the permeability. Examination of Fig. 3 shows that the refractive index has a negative real part $\mathrm{Re}(n_r)$ $[-1.5\leq\mathrm{Re}(n_r)\leq0]$ in the probe frequency detuning range $[0.25\gamma_-, 3.70\gamma_-]$. The bottom 35% of the detuning range has the lowest $\mathrm{Im}(n_r)$ values.

We conclude that, since the electric- and magnetic-dipole transitions of atoms can be excited by visible and infrared light, the refractive index of an atomic medium can display negative refractive behavior in a three-level dressed-state mixed-parity system at optical frequency bands. Viewed from a dressed-state perspective, some features not necessarily as obvious in a more conventional treatment (see [33] on a three-level system studying anisotropy with control and probe beams, and references therein pertaining to multilevel

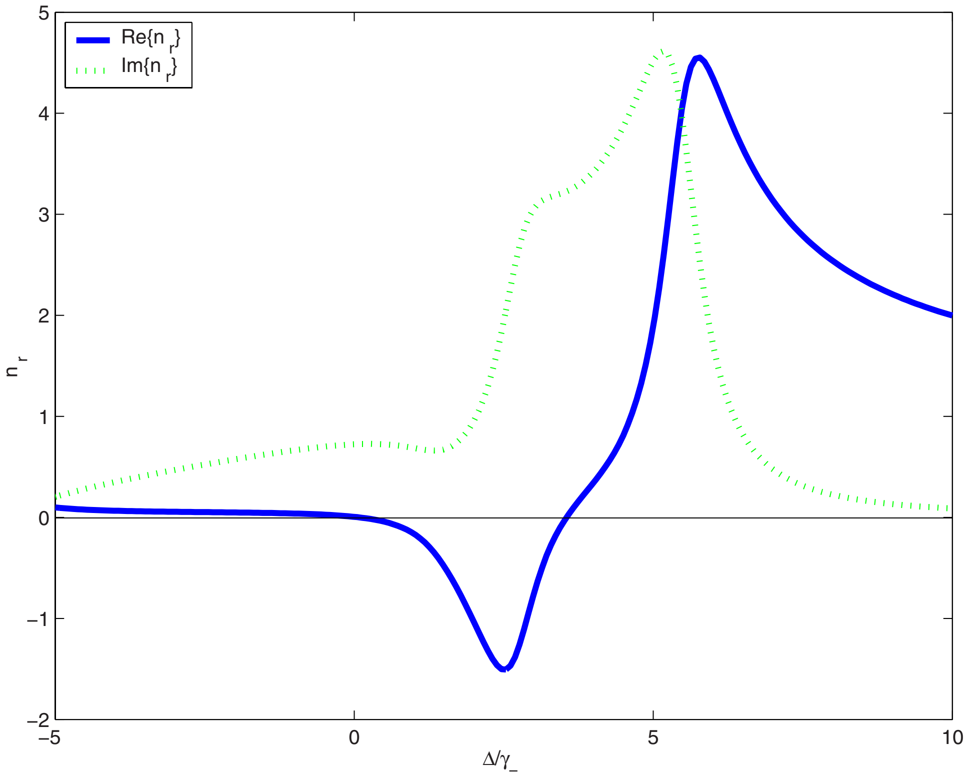

FIG. 3. (Color online) Dispersion behavior of the real and imaginary parts of the refractive index n_r, versus normalized detuning frequency Δ/γ_-, in the dressed-state mixed-parity medium.

systems) become apparent, such as the explicit display of parity mixing.

VII. CONCLUDING REMARKS

In this paper an approach has been presented to realize a negative refractive index employing dressed-state mixed-parity transitions of atoms. Expressions for the permittivity and permeability at the probe frequency have been provided, and numerical results given which demonstrate that an optically realizable left-handed medium can be obtained in an atomic vapor using selected parameter values. The approach should also be applicable to solid state media. Since there is no longer a paucity of left-handed media showing some promise of partial functioning in optical or near-optical bands, but still much work to be done on optimizing materials manufacturing and fabrication processes to control loss or other properties, with all of these methods employing macroscopic or nanoscopic processing, the work presented here may stimulate an interest in using atomic-scale microscopic structure units. Investigations into such atomic-scale materials may open studies of anomalous refraction and the testing of fundamental electromagnetic properties of negative index materials.

ACKNOWLEDGMENT

One of the authors (J.Q.S.) was supported by the Natural Science Foundation of China (Project No. 10604046).

APPENDIX A

Angle ϑ present in the dressed-state expressions for $|+\rangle$ and $|-\rangle$, defined in (14), is determined by obtaining the eigenmatrix solution of the EoM Hamiltonian $H_{\mathrm{equ}}^{\mathrm{EoM}}$ of (10). That is,

$$H_{\mathrm{equ}}^{\mathrm{EoM}}\begin{bmatrix}\alpha\\ \beta\end{bmatrix} = \begin{bmatrix}\hbar\delta/2 & V\\ V^* & -\hbar\delta/2\end{bmatrix}\begin{bmatrix}\alpha\\ \beta\end{bmatrix} = \lambda\begin{bmatrix}\alpha\\ \beta\end{bmatrix}. \tag{A1}$$

Equation (A1) requires the determinant of this homogeneous equation to be zero, or

$$\det\begin{bmatrix}\hbar\delta/2-\lambda & V\\ V^* & -\hbar\delta/2-\lambda\end{bmatrix} = 0, \tag{A2}$$

leading to

$$\lambda_\pm = \pm\frac{\hbar}{2}\sqrt{\delta^2+4|\Omega_{Rc}|^2}. \tag{A3}$$

Note that $|\Omega_{Rc}|^2=\Omega_R{}^2$. From the first row of (A1), the lower β element of the eigenvector is found as

$$\beta = -\frac{\hbar\delta/2-\lambda}{V}\alpha, \tag{A4}$$

and applying normalization

$$|\alpha|^2+|\beta|^2=1 \tag{A5}$$

yields

$$|\alpha|^2 = \frac{|\Omega_{Rc}|^2}{|\Omega_{Rc}|^2+(\delta/2+\lambda/\hbar)^2} = \frac{1}{2}\left(1\pm\frac{1}{\sqrt{1+4|\Omega_{Rc}|^2/\delta^2}}\right) \tag{A6}$$

with the extracted factor of $1/2$ arising from another squared Rabi frequency magnitude stored in the squared eigenvalue. The second eigenvector component is then

$$|\beta|^2 = \frac{1}{2}\left(1 \mp \frac{1}{\sqrt{1+4|\Omega_{Rc}|^2/\delta^2}}\right). \tag{A7}$$

Because the magnitudes of the eigenvector components are equal to or less than 1, assigning cosinusoids to them is acceptable; i.e.,

$$\alpha = \cos\vartheta e^{i\phi_\alpha}, \quad \beta = \sin\vartheta e^{i\phi_\beta}, \tag{A8a}$$

$$\cos\vartheta = \frac{1}{\sqrt{2}}\left[1 - \frac{1}{\sqrt{1+4|\Omega_{Rc}|^2/\delta^2}}\right]^{1/2},$$

$$\sin\vartheta = \frac{1}{\sqrt{2}}\left[1 + \frac{1}{\sqrt{1+4|\Omega_{Rc}|^2/\delta^2}}\right]^{1/2}, \tag{A8b}$$

which implicitly contains two solutions $\{\alpha_+,\beta_+\}$, $\{\alpha_-,\beta_-\}$ utilized in (11):

$$\alpha_+ = \cos\vartheta e^{i\phi_{\alpha_+}}, \quad \beta_+ = \sin\vartheta e^{i\phi_{\beta_+}}, \tag{A9a}$$

$$\alpha_- = \cos\vartheta e^{i\phi_{\alpha_-}}, \quad \beta_- = \sin\vartheta e^{i\phi_{\beta_-}}. \tag{A9b}$$

One can rewrite (A8b), identifying $|\Omega_{Rc}|^2 = \Omega_R{}^2 = R_0{}^2$, as

$$\cos\vartheta = \frac{1}{\sqrt{2}}\sqrt{\frac{R-\delta}{R}}, \quad \sin\vartheta = \frac{1}{\sqrt{2}}\sqrt{\frac{R+\delta}{R}}, \quad R = \sqrt{\delta^2 + R_0{}^2}. \tag{A10}$$

Using (A10), the 2ϑ cosinusoidal results are

$$\cos 2\vartheta = \cos^2\vartheta - \sin^2\vartheta = -\frac{\delta}{R},$$

$$\sin 2\vartheta = 2\cos\vartheta \sin\vartheta = \frac{R_0}{R}, \tag{A11}$$

and these are the same identifications as in [30]. The assignments for $\cos\vartheta$ and $\sin\vartheta$ in (A8b) according to (A7) assure a negative sign in the former and a positive sign in the latter.

Angles of α_+ and α_- are determined by referring to the solution (derived in Appendix B) when $\phi=0$ [see (5)], which is

$$\alpha_\pm/\cos\vartheta = \pm 1, \tag{A12}$$

yielding

$$\phi_{\alpha_\pm} = 2n_+\pi, (2n_- - 1)\pi, \tag{A13}$$

where $n=n_+, n_-$ are any integers. The angles of β_+ and β_- are determined by inserting α_+ and α_- into (A4) and retrieving V from (5). This generates

$$\beta_\pm = -\frac{\hbar\delta/2 \mp \frac{\hbar}{2}\sqrt{\delta^2 + 4|\Omega_{Rc}|^2}}{\hbar\Omega_R e^{i\phi}/2}\alpha_\pm, \tag{A14}$$

which produces

$$\phi_{\beta_\pm} = -\phi. \tag{A15}$$

It is noted that (A15) automatically satisfies the $\phi=0$ solution,

$$\beta_\pm/\sin\vartheta = 1. \tag{A16}$$

APPENDIX B

The equation of motion equation in [30] ($H^{\text{EoM}}_{\text{equ}} = -\hbar M/2$) is similar to but distinct from (A1) and has the appearance ($H^{\text{EoM}}_{\text{equ}} = \hbar M/2$)

$$M\begin{bmatrix} u \\ v \end{bmatrix} = \begin{bmatrix} \delta & R_0 \\ R_0 & -\delta \end{bmatrix}\begin{bmatrix} u \\ v \end{bmatrix} = \lambda\begin{bmatrix} u \\ v \end{bmatrix}. \tag{B1}$$

Again, this equation's eigenvalues are determined, by the procedure in Appendix A, to be

$$\lambda = \pm R. \tag{B2}$$

From the second row in (B1),

$$u = \frac{\lambda - \delta}{R_0}v. \tag{B3}$$

Normalizing the eigenvector using

$$u^2 + v^2 = 1 \tag{B4}$$

provides

$$v = \pm\frac{R_0}{\sqrt{(\lambda-\delta)^2 + R_0{}^2}}. \tag{B5}$$

Enlisting (B3), u is found as

$$u = \pm\frac{\lambda - \delta}{\sqrt{(\lambda-\delta)^2 + R_0{}^2}}. \tag{B6}$$

Choosing the positive sign, the eigenvector for $\lambda_2 = R$ may be expressed in the form

$$\begin{bmatrix} u_2 \\ v_2 \end{bmatrix} = \frac{1}{\sqrt{(R-\delta)^2 + R_0{}^2}}\begin{bmatrix} R-\delta \\ R_0 \end{bmatrix}. \tag{B7}$$

From the first row in (B1),

$$u = \frac{R_0}{\delta + \lambda}, \tag{B8}$$

and again applying (B4),

$$v = \pm\frac{(\delta+\lambda)}{\sqrt{R_0{}^2 + (\delta+\lambda)^2}}. \tag{B9}$$

Choosing the positive sign, the eigenvector for $\lambda_2 = -R$ may be expressed in the form

$$\begin{bmatrix} u_1 \\ v_1 \end{bmatrix} = \frac{1}{\sqrt{R_0{}^2 + (\delta - R)^2}}\begin{bmatrix} R_0 \\ \delta - R \end{bmatrix}. \tag{B10}$$

The eigenvector forms in (B7) and (B10) agree with those in [30].

Following the procedure in (11)–(13), with $M' = U_d^{-1}MU_d$ diagonalizing M by using a unitary matrix U_d, with U_d found as [27]

$$U_d = \left[\begin{pmatrix} u_2 \\ v_2 \end{pmatrix} \begin{pmatrix} u_1 \\ v_1 \end{pmatrix} \right] = \left[\begin{pmatrix} \cos \vartheta \\ \sin \vartheta \end{pmatrix} \begin{pmatrix} -\sin \vartheta \\ \cos \vartheta \end{pmatrix} \right] \tag{B11}$$

with the dressed $\phi=0$ wave function coefficients being expressible as

$$\begin{bmatrix} C_+(t) \\ C_-(t) \end{bmatrix} = U \begin{bmatrix} C_a(t) \\ C_b(t) \end{bmatrix}, \quad U = U_d^{-1} = U_d^{\dagger}, \tag{B12}$$

which can be restated as

$$|+\rangle = \cos \vartheta |a\rangle + \sin \vartheta |b\rangle,$$

$$|-\rangle = -\sin \vartheta |a\rangle + \cos \vartheta |b\rangle. \tag{B13}$$

APPENDIX C

Hamiltonian in (31) may be written more compactly as

$$H' = \hbar \omega_{-g} \sigma_z/2 + \hbar(a^{\dagger}a + 1/2) + \begin{bmatrix} 0 & -\wp_{-g}E_p^Q(t) - \mathscr{m}_{-g}B_p^Q(t) \\ -\wp_{g-}E_p^Q(t) - \mathscr{m}_{g-}B_p^Q(t) & 0 \end{bmatrix} \tag{C1}$$

by eliminating the diagonal H_1^{em} elements by symmetry. Referring to the last term in (C1) as $H_1'^{\mathrm{em}}$, it may be cast as

$$H_1'^{\mathrm{em}} = \hbar(\bar{\Omega}_p^Q \sigma_+ + \bar{\Omega}_p^{Q*} \sigma_-)(a + a^{\dagger}), \tag{C2}$$

where

$$\Omega_p^Q = 2\sqrt{n+1}\bar{\Omega}_p^Q,$$

$$\Omega_p^{QE} = 2\sqrt{n+1}\bar{\Omega}_p^{QE}, \quad \Omega_p^{QB} = 2\sqrt{n+1}\bar{\Omega}_p^{QB}. \tag{C3}$$

For Ω_p^Q real, (C2) becomes

$$\begin{aligned} H_1'^{\mathrm{em}} &= \hbar \bar{\Omega}_p^Q (\sigma_+ + \sigma_-)(a + a^{\dagger}) \\ &= \hbar \bar{\Omega}_p^Q [(a\sigma_+ + a^{\dagger}\sigma_-) + (a\sigma_- + a^{\dagger}\sigma_+)] \\ &= \hbar \bar{\Omega}_p^Q \{[a(0)\sigma_+(0)e^{i\Delta t} + a^{\dagger}(0)\sigma_-(0)e^{i\Delta t}] \\ &\quad + [a(0)\sigma_-(0)e^{-i(\omega_p+\omega_{-g})t} + a^{\dagger}(0)\sigma_+(0)e^{i(\omega_p+\omega_{-g})t}]\} \\ &= \hbar \bar{\Omega}_p^Q (a\sigma_+ + a^{\dagger}\sigma_-), \end{aligned} \tag{C4}$$

where the last equality came from applying the rotating wave approximation, and the third arose from working entirely in the Heisenberg picture where a and $a^{\dagger}$ have previously incorporated the variation. The Pauli spin raising and lowering operators similarly derive from $d\sigma_{\pm}(t)/dt = (i/\hbar)[\hbar\omega_{-g}\sigma_z/2, \sigma_{\pm}] + U_{\ell 2}^{\dagger} \partial \sigma_{\pm}/\partial t U_{\ell 2}$, with $U_{\ell 2} = e^{-H_{0L}t/\hbar}$ and explicit time variation absent, giving $\sigma_{\pm}(t) = \sigma_{\pm}(0)e^{\pm i\omega_{-g}t}$.

Therefore,

$$H' = \hbar \omega_{-g} \sigma_z/2 + \hbar(a^{\dagger}a + 1/2) + \hbar \bar{\Omega}_p^Q (a\sigma_+ + a^{\dagger}\sigma_-), \tag{C5}$$

which can be evaluated in the $|-n\rangle - |g(n+1)\rangle$ manifold to be

$$H' = \hbar(n+1)\omega_p \begin{bmatrix} 1 & 0 \\ 0 & 1 \end{bmatrix} + \frac{\hbar}{2} \begin{bmatrix} \Delta & 2\bar{\Omega}_p^Q\sqrt{n+1} \\ 2\bar{\Omega}_p^Q\sqrt{n+1} & -\Delta \end{bmatrix}. \tag{C6}$$

The Hamiltonian in (C6) can be diagonalized to obtain the manifold $|-n\rangle - |g(n+1)\rangle$ states, and the eigenenergies are

$$E_{-n} = \hbar(n+1)\omega_p + \frac{\hbar}{2}\sqrt{\Delta^2 + 4\bar{\Omega}_p^{Q^2}},$$

$$E_{g(n+1)} = \hbar(n+1)\omega_p - \frac{\hbar}{2}\sqrt{\Delta^2 + 4\bar{\Omega}_p^{Q^2}}. \tag{C7}$$

[1] V. G. Veselago, Sov. Phys. Usp. **10**, 509 (1968).
[2] R. A. Shelby, D. R. Smith, and S. Shultz, Science **292**, 77 (2001).
[3] J. B. Pendry, Phys. Rev. Lett. **85**, 3966 (2001).
[4] A. Lakhtakia, M. W. McCall, and W. S. Weiglhofer, in *Introduction to Complex Mediums for Optics and Electromagnetics*, edited by W. S. Weiglhofer and A. Lakhtakia (SPIE Press, Bellingham, WA, 2003), p. 347.
[5] L. Chen, S. He, and L. Shen, Phys. Rev. Lett. **92**, 107404 (2004).
[6] A. Lakhtakia, AEU, Int. J. Electron. Commun. **58**, 229 (2004).
[7] A. Lakhtakia, Opt. Express **11**, 716 (2003).
[8] J. Q. Shen, Phys. Lett. A **344**, 144 (2005).
[9] Z. M. Zhang and C. J. Fu, Appl. Phys. Lett. **80**, 1097 (2002).
[10] C. M. Krowne, Phys. Rev. Lett. **92**, 053901 (2004).
[11] C. M. Krowne, J. Appl. Phys. **99**, 044914 (2006).
[12] J. B. Pendry, A. J. Holden, D. J. Robbins, and W. J. Stewart, J. Phys.: Condens. Matter **10**, 4785 (1998).
[13] J. B. Pendry, A. J. Holden, W. J. Stewart, and I. Youngs, Phys. Rev. Lett. **76**, 4773 (1996).
[14] C. R. Simovski and S. He, Phys. Lett. A **311**, 254 (2003).
[15] J. Q. Shen, Ann. Phys. **13**, 335 (2004).
[16] D. R. Smith, W. J. Padilla, D. C. Vier, S. C. Nemat-Nasser, and S. Schultz, Phys. Rev. Lett. **84**, 4184 (2000).
[17] R. A. Shelby, D. R. Smith, S. C. Nemat-Nasser, and S. Schultz, Appl. Phys. Lett. **78**, 489 (2001).
[18] L. B. Hu and S. T. Chui, Phys. Rev. B **66**, 085108 (2002).
[19] S. He, Z. C. Ruan, L. Chen, and J. Q. Shen, Phys. Rev. B **70**, 115113 (2004).
[20] A. Berrier, M. Mulot, M. Swillo, M. Qiu, L. Thylén, A. Talneau, and S. Anand, Phys. Rev. Lett. **93**, 073902 (2004).
[21] M. Notomi, Phys. Rev. B **62**, 10696 (2000).
[22] S. Treyakov, I. Nefedov, A. Sihvola, S. Maslovski, and C. Simovski, J. Electromagn. Waves Appl. **17**, 695 (2003).
[23] J. Pendry, Science **306**, 1353 (2004).
[24] T. G. Mackay, Microwave Opt. Technol. Lett. **45**, 120 (2005).
[25] T. G. Mackay and A. Lakhtakia, Phys. Rev. E **69**, 026602 (2004).

[26] G. V. Eleftheriades, A. K. Iyer, and P. C. Kremer, IEEE Trans. Microwave Theory Tech. **50**, 2702 (2002).
[27] C. M. Krowne, in *Advances in Imaging and Electron Physics*, edited by Peter W. Hawkes (Academic Press, San Diego, 1996), Vol. 98, pp. 77–321.
[28] S. John and M. Florescu, J. Opt. A, Pure Appl. Opt. **3**, S103 (2001).
[29] E. Forsberg, B. Hessmo, and Lars Thylen, IEEE J. Quantum Electron. **40**, 400 (2004).
[30] P. Meystre and M. Sargent III, *Elements of Quantum Optics*, 3rd ed. (Springer-Verlag, Berlin, 1998), Chaps. 3 and 5.
[31] M. O. Scully and M. S. Zubairy, *Quantum Optics* (Cambridge University Press, Cambridge, U.K., 2001).
[32] C. M. Krowne, Phys. Lett. A **372**, 2304 (2008).
[33] C. M. Krowne, Phys. Lett. A **372**, 3926 (2008).